NUMERICAL MODELING OF THE LOAD-DEFORMATION BEHAVIOR OF DOWELED SOFTWOOD AND HARDWOOD JOINTS

*Alfredo Manuel Pereira Geraldes Dias**

Assistant Professor
Department of Civil Engineering
University of Coimbra
Coimbra, Portugal

Jan Willem Van de Kuilen

Professor
Technical University of Munich
Munich, Germany
Delft University of Technology
Delft, The Netherlands

Helena Maria Pires Cruz

Senior Research Officer
LNEC
Lisbon, Portugal

Sergio Manuel Rodrigues Lopes

Associate Professor
Department of Civil Engineering
University of Coimbra
Coimbra, Portugal

(Received April 2010)

Abstract. This article presents a nonlinear finite element model developed to simulate the load-deformation behavior of wood joints when loaded by a dowel-type fastener. Particular attention was paid to the initial load-deformation behavior that had a significant influence on the joint stiffness, a joint property with a large influence on the mechanical behavior of wood-based composite structures connected with semirigid joints. To obtain accurate predictions of joint deformation, the material models available in the literature were adapted and nonlinear deformations were taken into consideration during very early loading. The proposed model precisely describes the embedding behavior of different wood species and densities. Numerical results compared very well with those obtained in experiments. Based on this analysis, the recommendation is to obtain the material model inputs based on design values available in the literature.

Keywords: Constitutive law, dowel-type fasteners, finite elements method, nonlinear analysis, wood joints, yield criterion.

INTRODUCTION

The use of nonlinear finite element models (FEM) has been increasingly used to predict mechanical behavior of wood joints. This simulation has significant advantages compared with other modeling approaches and experimental assessments, providing a better understanding of the mechanical phenomena. Once the models are developed and validated, very simple analysis of new conditions and situations is possible and expensive verification with laboratory tests is reduced. A key point of the modeling is the material constitutive models. The mechanical behavior of wood joints with slender dowel-type fasteners is characterized by compression

* Corresponding author: alfgdias@dec.uc.pt

stresses associated with large plastic deformations. Various models have been used to simulate this behavior for wood.

Patton-Mallory et al (1997) proposed an FEM for bolted joints made with Douglas-fir and western hemlock. The steel was modeled as an elastic perfectly plastic material. Wood was modeled based on an orthotropic constitutive law considering trilinear wood compression behavior and trilinear shear stiffness degradation. The plastic criterion considered independent behavior in the three orthotropic directions. Numerical results showed a more rigid behavior than that of the experiments attributed to disregarding the degradation of perpendicular-to-grain tension stiffness. Nevertheless, the model displayed important characteristics found in the experiments. It was also found that the model was insensitive to the method of determining symmetric pairs of Poisson's ratios (ν_{23}, ν_{32}).

Chen et al (2003) presented another nonlinear 3D FEM to predict load-carrying capacity of dowel-type joints made with spruce unreinforced and reinforced with fiberglass. In this work, a plane stress analysis was performed. The failure criterion was based on two critical material strengths, tensile stress perpendicular to the grain and shear stress parallel to the grain. To obtain better predictions of the initial load-slip behavior, the modulus of elasticity in the crushed area was considered as one-half of that of remaining areas. The authors found good agreement between the numerical and experimental values of load-carrying capacity of the joints.

Adalian (2002) developed a model to simulate the behavior of shock absorbers made of poplar. Uniaxial tests were performed to assess the static and dynamic mechanical behavior of the wood. Based on these tests, empirical laws were proposed based on the density and initial geometry of the test sample. The plasticity criterion considered independent behavior in the three orthotropic directions. For longitudinal compression, the stress–strain included a peak in the limit of the linear elastic phase followed by yielding without increasing the stresses after which there is a significant increase in the stress "consolidation phase" caused by material densification.

To model wood with coupled material behavior in the three directions, Kharouf et al (2003) used Hill yield criteria (Hill 1950). Spruce wood bolted joints were simulated assuming elastic perfectly plastic material for wood. Reasonable agreements were found between numerical simulations and experimental measurements of local and global deformations. The prediction precision increased with the load applied; for lower load levels, the numerical simulations tended to underestimate the experimental deformations. Furthermore, the predicted failure modes were found to be consistent with experimental observations.

The validation of these models has been focused on load-carrying capacity, largely resulting in simulations with underestimations of the initial deformations of the load-slip assumed to be linear elastic. These initial deformations define the joint stiffness, which in certain situations (eg composite structures connected with semirigid joints) is a key parameter in structural design, as shown by several authors (Fragiacomo et al 2007; Gutkowski et al 2008; Dias et al 2010). Recent studies (Dias 2006; Dias et al 2007b) showed that an accurate simulation of the initial joint behavior cannot be obtained assuming an elastic or even elastic perfectly plastic behavior for wood.

All developed models were tested on a limited number of wood species (always softwoods and mostly spruce) and it remains unclear if they can be extrapolated to other species with different densities. Furthermore, the mechanical properties necessary to define the material constitutive laws are usually based on the design values available in the literature (eg Wood Handbook [FPL 1999]). This approach was followed by Dias et al (2007b) with a reasonable prediction in modeling the mechanical behavior of doweled wood–concrete joints. However, there were some important differences between the numerical and experimental results apparently caused by two main reasons: natural variation of wood material properties, even for the same

species; and, especially, the direct input of design values from the literature, meant for purposes other than finite element modeling, into the constitutive models. It was concluded that the numerical description of joint behavior could be significantly improved with better relationships between the design properties and the input properties of the constitutive models.

In this work, a yield criterion complying with the laws of the constitutive modeling in continuum media (Hill 1950), with coupled material behavior in each direction, was used to model the mechanical behavior of wood. Because the models traditionally used are not able to describe initial deformation, a new elastic-plastic behavior was developed. A number of improvements were introduced to the previously proposed models to have accurate predictions for high and low load levels as well as for a complete unloading–reloading cycle. This constitutive material model was used to simulate a large number of embedment tests performed in accordance with the European Standard EN 383 (CEN 1993). This standard indicates the methods and principles to determine the embedment properties (strength and stiffness) of wood. The simulations were performed for three materials: two softwoods, spruce and Maritime pine, and one hardwood, chestnut. Furthermore, the specimens selected were from a wide range of densities, 380-715 kg/m^3. From the analysis of these results it was possible to provide relationships between design properties and FEM constitutive material properties.

EMBEDMENT TESTS AND MODELS

The preparation and performance of the embedment tests followed the procedures defined in EN 383 (CEN 1993). The test specimens were obtained from spruce, Maritime pine, and chestnut as described in Dias et al (2007a). The wood specimens were conditioned to 12% EMC at 20°C ± 5% and 65% ± 5% RH. Mean values of the density from the three wood species were 455, 566, and 605 kg/m^3 for spruce, chestnut, and maritime pine, respectively. The fastener used in the tests was a 10-mm-dia steel dowel. Specimen configuration is given in Fig 1. The specimen was 140 mm (longitudinal) and 20 × 60 mm in cross-section with random radial and tangential orientation. The dowel was inserted in 10-mm-dia predrilled holes to ensure a tight fit.

A number of difficulties were found in obtaining tight-fitting holes on spruce test specimens, because there was always some clearance and parts of the fibers were not cut, but crushed, leading to imperfect surfaces and damage to the surrounding fibers (Dias 2005).

During the test, the load was measured at one point using a single load cell and the displacements were measured every sec at two points

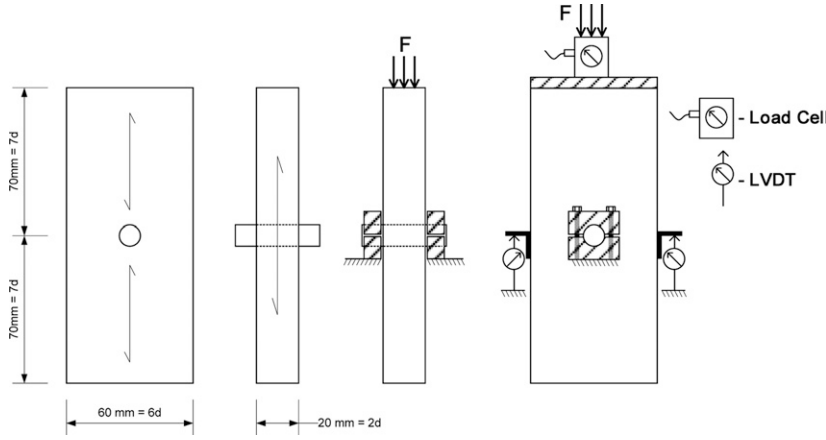

Figure 1. Test specimen configuration and test setup.

using LVDTs (Fig 1). The loading was applied as prescribed in EN 383 with an unloading–reloading stage at 10-40% of the expected maximum load.

Generally, the load-slip curve began with a relatively linear initial portion compared with the load-slip obtained for later stages. For a slip at about 1 mm, the rate of loading decreased, remaining relatively constant. According to EN 383, the load-carrying capacity is the maximum load reached during the deformation to 5 mm or, alternatively, the load measured at 5 mm. In these tests, the load usually increased up to 5 mm; however, in some cases, there was a slight yield drop before the 5-mm deformation. These yield drops defined the maximum load and consequently the load-carrying capacity. Most of the test specimens had an initial slip caused by the hole clearance, therefore even "tight-fitting" dowels will show some initial slip.

In a few tests, failure occurred from premature splitting of the wood, causing a substantial decrease in the load. These splits were usually initiated at an existing defect, typically a small check, possibly caused by drying to 12% EMC as required by EN 383. In many other tests, splits were also formed below the fastener. These occurred during the test but did not increase sufficiently to cause failure. In fact, the loads and deformations that were observed were similar to those in specimens without visible splits. This led to the conclusion that such splits did not lead to failure and apparently did not influence the load-slip behavior. The load-slip behavior of the test specimens was relatively linear to the yielding phase followed by a nearly constant but slowly increasing load. The shape of the curves was very similar to the stress-deformation curve of a material with an elastic perfectly plastic behavior.

Figure 2 depicts the mesh used to simulate the mechanical behavior of wood in the embedment tests based on preliminary calculations using various mesh configurations. The final mesh (Fig 2) was selected based on the precision of the models and their numerical stability as described by Dias (2006).

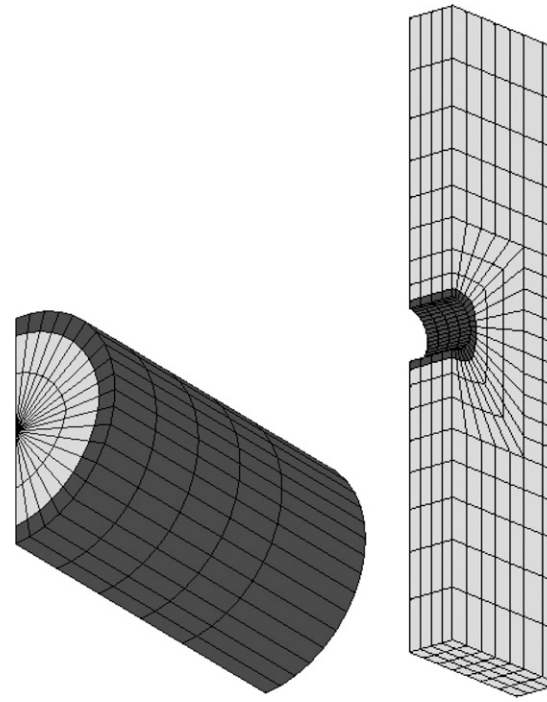

Figure 2. Embedding model mesh and contact elements.

Support conditions were simulated assuming zero translation in the three directions for all nodes in the bottom plane of the model. The load was applied to the nodes of the lateral surface of the dowel and in the simulations without cycling it consisted of a controlled displacement. In the experiments, the load was applied on the wood member and the dowel ends were fixed (supports). Despite such apparent differences between the modeling boundary conditions and test load and support conditions, the displacement measured was exactly the same. The measured displacement was the relative deformation between the height of the dowel on the fastener and the wood for the equivalent stress fields. Load cycles were simulated through the application of a face load applied on the lateral surface of the dowel following the procedure of EN 383.

The interaction surfaces between wood and steel were modeled using deformable contact elements. Friction was modeled using the Coulomb stick-slip model with a 0.5 friction coefficient for wood–steel (Dias et al 2007b).

For elastic behavior, wood was modeled as an orthotropic material. The relations between the elastic moduli in the various directions and between elastic and shear moduli were kept constant as specified in EN 338 (CEN 2003).

Direction *xx* is the direction parallel to the fibers; the other two principal directions are *yy* and *zz*. No distinction in orientation or values was made between *yy* and *zz* directions, each being considered perpendicular to the grain.

For plastic behavior, the orthotropic yield criteria associated with isotropic hardening proposed by Hill (1950) were used.

In the initial approach, the mechanical behavior of wood was assumed to be elastic perfectly plastic (Fig 3: bilinear). This stress–strain behavior was later improved by assuming nonlinear deformations from close to the start of the test (Fig 3: trilinear) at a stress level corresponding to 0.16 of the yield stress ($\bar{\sigma}$). It was assumed that the initial adjustments between steel and wood (eg hole clearance) had already occurred. These nonlinear deformations may represent small amounts of stick-slip friction between the fastener and surrounding wood at the initial stage or even material densification in the area adjacent to the dowel where high stress concentrations occur. These phenomena are caused by many factors that are difficult to model, eg the material density, characteristics of the drilling tools, or even the drilling procedure. In this research only the wood density was taken into account with other factors kept constant; they are usually rather variable in practice and therefore difficult to model.

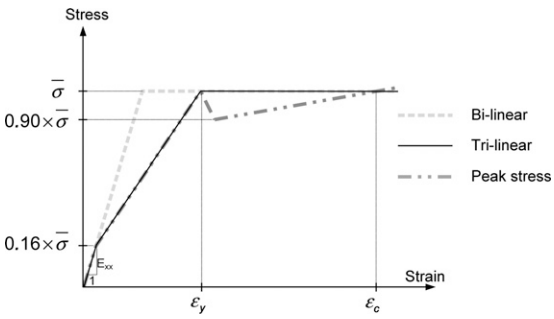

Figure 3. Stress–strain diagrams for wood.

A further improvement (Fig 3: peak stress) was introduced by assuming a yield drop in the stress–strain curve, as described by Van der Put (1989) and also in the constitutive model proposed by Adalian (2002).

The ratios between yield stress parallel to the grain and yield stress ($\sigma_0/\bar{\sigma}$), yield stress perpendicular to the grain and yield stress ($\sigma_{90}/\bar{\sigma}$), yield shear stress and yield stress ($\sqrt{3}\sigma_v/\bar{\sigma}$) were fixed at 1.0, 0.19, and 0.38, respectively. A detailed analysis of these ratios was performed by Dias (2006) where a parametric analysis was used to assess the influence of these ratios on stresses and deformations. The values used here were those that provided the most accurate description of the loads and deformations observed in experiments. Therefore, it was concluded in that study that these values led to the best description of wood material behavior.

The material behavior of the steel was simulated assuming an isotropic constitutive law and an isotropic yield criterion of von Mises (Silva 2006). The mechanical properties of steel were obtained from tension tests on round steel bars (Dias 2005).

NUMERICAL SIMULATIONS OF EMBEDMENT TESTS

From the material properties of wood, the only property clearly known for each of the test specimens was density, but that is not sufficient to define all the other properties with the required precision. Subsequently, the first attempt was based on density, which was improved iteratively by comparing the results of simulations with data from embedment tests. The initial values used in the simulations were the same in each test series (Table 1).

The first simulations on the basis of elastic perfectly plastic behavior clearly showed that the initial stiffness of the joints had a weak relationship with elastic properties. The models significantly underestimated the deformations measured in the embedment tests. Variations in elastic modulus of 8-12 GPa were made. However,

Table 1. Initial values for wood properties in the simulations.

Species	ρ (kg/m^3)	E_{xx} (GPa)	$\bar{\sigma}$(MPa)	ε_y	ε_c
Spruce	447	9	33.0	0.004	1.0
Chestnut	591	10	42.0	0.004	1.0
Maritime pine	640	12	45.0	0.004	1.0

to obtain numerical deformations comparable with test values, the elastic properties had to be reduced significantly, in some simulations to 4 GPa, but these values clearly lack physical meaning. This indicates that modeling the behavior of fasteners and holes requires additional parameters or means of modeling that cannot be achieved on the basis of standard material parameters and geometry modeling. Clearly, the interaction between the elements in the model did not represent the actual behavior of the material and corresponding stresses and strains. The effect was very significant for spruce. However, its importance decreased with an increase of wood density. In higher-density specimens of all three species, the initial deformations predicted by the model assuming linear elastic behavior are similar to those obtained from tests.

These results gave a strong indication that the mechanical behavior of wood in the embedment tests was influenced by nonlinear deformations in the initial loading. To take that into account, the bilinear stress–strain behavior was upgraded to trilinear (Fig 3), significantly improving the precision of the predictions.

Despite the results obtained with the trilinear model, further efforts were made to improve it by introducing a yield drop (peak stress model). The results obtained for one of the specimens simulated with the three constitutive material models of wood (bilinear, trilinear, peak stress) are given in Fig 4. The comparison of the test curve with the three numerical simulations shows that the use of the peak stress model led to the most precise predictions, particularly for the test specimens with a very pronounced yield point. However, because of the yield drop in the stress–strain diagram, the calculations became more time-consuming and unstable. From the analysis of the precision intended in this type

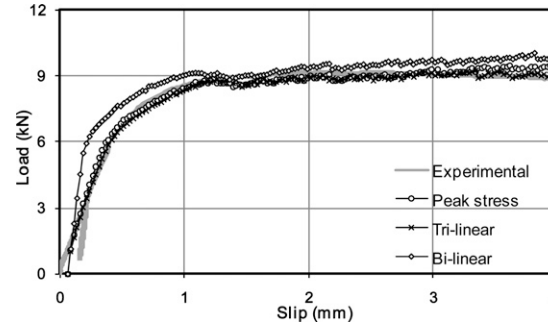

Figure 4. Experimental result and numerical simulations with the three material constitutive models.

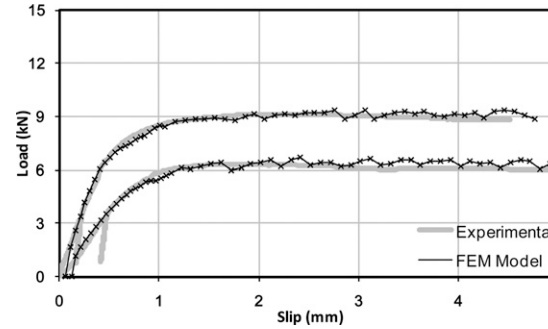

Figure 5. Finite element model simulation for spruce.

of simulation and the extra efforts required by the use of a more sophisticated model, it was decided to continue the simulations using the trilinear model, which led to results nearly almost as good as the peak stress model.

Figures 5-7 show the experimental and numerical load-slip curves for two test specimens from each species (those with low and high embedding strength) where the numerical results were very similar to test data. This is supported by the stress analysis plotted in Fig 8 for one simulation. The locations where the maximum stresses (compression parallel and tension perpendicular to the grain) were obtained in the numerical simulations correspond to those where wood crushing and splitting were observed.

Nevertheless, in the very early stages of the load-slip curves, there are still differences. This may be from hole clearance and similar imperfections

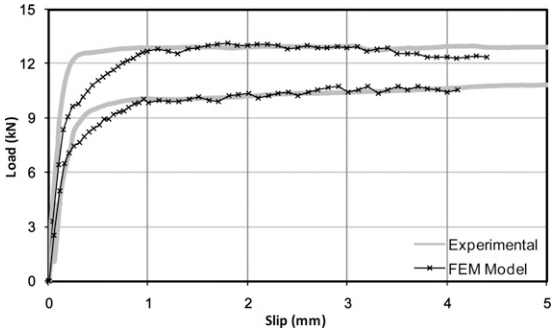

Figure 6. Finite element model simulation for chestnut.

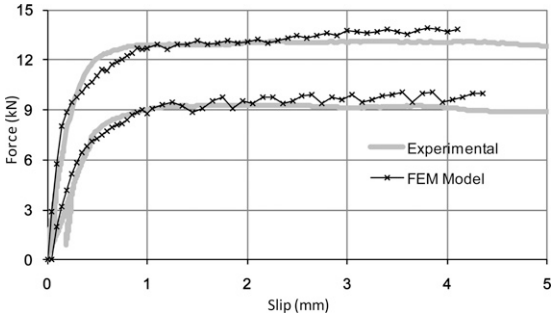

Figure 7. Finite element model simulation for Maritime pine.

that could not be avoided, particularly for the test specimens of lower-density wood. Such imperfections might lead to initial deformations that the model did not take into account. In the test with this type of deformation it was decided to add it to the slip values obtained in the simulations. For this reason, the numerical curves do not start at the origin in some of the simulations.

Further simulations were performed to evaluate the precision of the trilinear model simulating the unloading–reloading cycle obtained in the tests performed in accordance with EN 383 and EN 26891 (CEN 1991). The results of two simulations (corresponding to hardwoods with yield strain, ε_y, of 0.009 and softwoods with $\varepsilon_y = 0.034$) are given in Fig 9.

These results show that the model proposed simulates the mechanical behavior of wood very precisely, even for loading and unloading cycles. Furthermore, these simulations confirm that the initial relatively low stiffness can be precisely predicted through the consideration of elastic-plastic behavior from the initiation of loading. The cycle simulation shows that this approach represents the material behavior more

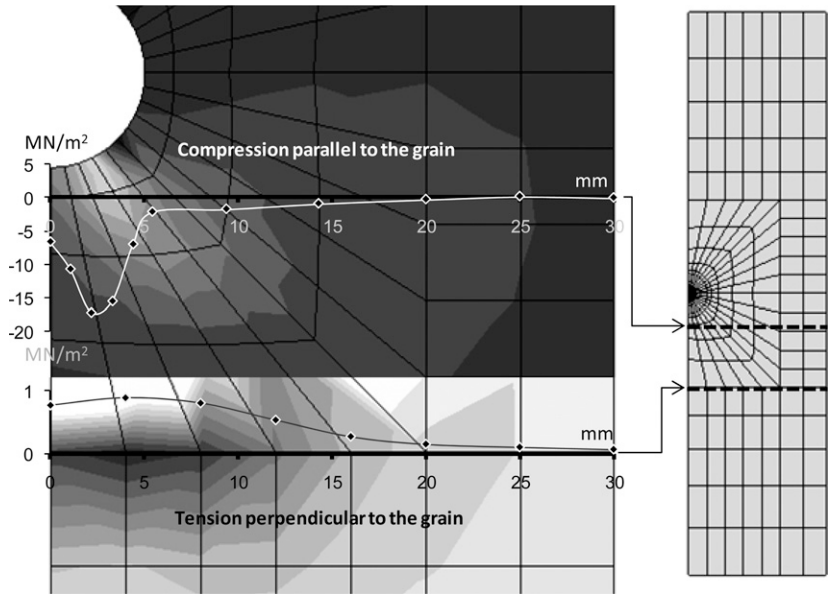

Figure 8. Compression parallel and tension perpendicular to the grain for an embedment test simulation.

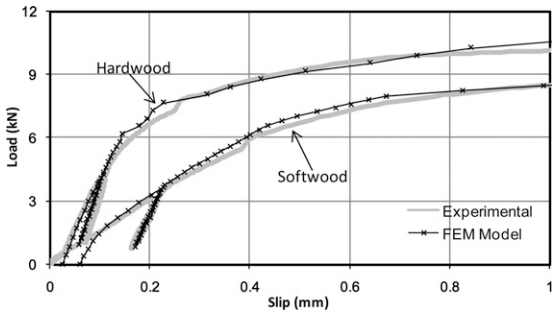

Figure 9. Finite element model simulation of the unloading–loading cycle.

precisely than assuming unrealistic low elasticity properties. In the cycle, the stiffness increased once it was not further influenced by nonlinear deformations that occurred in the initial uploading.

The comparison between measured and predicted deformation in the cycle also indicates that the elastic properties found in the literature, eg the Wood Handbook (FPL 1999), can successfully be used for FEM modeling if combined with appropriate yield criteria and hardening rules.

Once the global load-slip curve was simulated for a typical embedment test, a larger number of tests was used to obtain constitutive models valid for wider ranges of wood species with different density ranges that could be used for analyses with different types of joints. These test specimens were selected on a random basis to cover a range of wood species and densities of 380-715 kg/m^3.

The values of the material properties used in the simulations are given in Table 2. In Fig 10, yield stress is plotted as a function of the wood-embedding strength. Yield stress increases approximately proportionally to the embedding strength, being lower than the embedding strength but higher than the expected compression strength, in agreement with Dias et al (2007b). From these results the following relationship between theoretical yield stress ($\bar{\sigma}$) and embedding strength (f_h) for the Hill criterion

Table 2. Stress and strains used in the simulations.

	Experimental tests						Numerical models			
	Density (kg/m^3)		Embedding strength (MPa)		Foundation modulus (GPa/m)		Yield stress (MPa)		Yield strain	
Species		Mean		Mean		Mean		Mean		Mean
Spruce	380	446	31.3	40.5	44.1	71.0	27.3	32.1	0.053	0.065
Spruce	386		33.9		58.7		29.0		0.128	
Spruce	401		32.2		61.5		27.3		0.063	
Spruce	424		37.0		49.5		29.1		0.073	
Spruce	436		39.4		56.1		32.0		0.074	
Spruce	449		38.3		50.4		32.0		0.104	
Spruce	450		43.6		100.3		33.7		0.024	
Spruce	474		52.4		93.8		44.0		0.035	
Spruce	479		37.0		66.0		29.0		0.073	
Spruce	499		45.4		83.5		33.7		0.034	
Spruce	525		55.6		117.5		36.0		0.054	
Chestnut	533	591	49.3	52.7	209.2	237.7	36.4	38.4	0.014	0.007
Chestnut	565		52.0		236.2		39.0		0.009	
Chestnut	576		54.8		188.5		42.0		0.004	
Chestnut	599		53.7		176.9		38.2		0.014	
Chestnut	627		54.8		303.0		36.4		0.004	
Chestnut	647		51.6		312.3		38.2		0.004	
Maritime pine	566	640	43.2	54.9	71.7	180.7	35.0	41.4	0.053	0.025
Maritime pine	574		45.6		93.1		33.7		0.023	
Maritime pine	598		54.7		150.0		45.0		0.044	
Maritime pine	677		65.1		333.0		47.3		0.004	
Maritime pine	710		55.9		147.2		40.0		0.013	
Maritime pine	715		64.5		289.1		47.3		0.014	

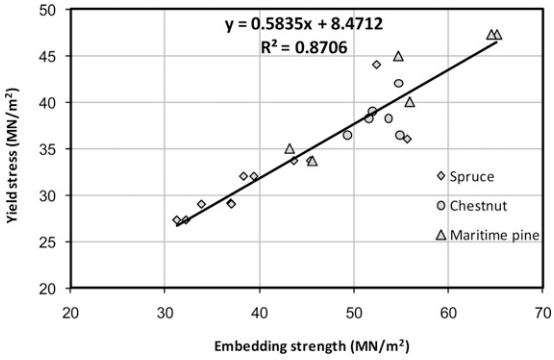

Figure 10. Relationship between yield stress and embedding strength of three species.

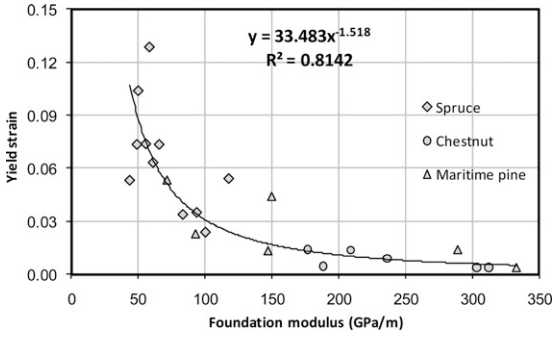

Figure 11. Relationship between yield strain and foundation modulus of three species.

(Hill 1950) can be determined independently of the wood species by:

$$\bar{\sigma} = 0.58 f_h + 8.5 \qquad (1)$$

In Fig 11, yield strain, ε_y, is plotted against foundation modulus, which is calculated as the ratio between 40% of the maximum estimated load-carrying capacity and the deformation measured for that load. This property is closely connected with the embedding stiffness of wood. The graph clearly shows that nonlinear deformations occurring from the initiation of the embedment test significantly influence the initial stiffness. The importance of this effect increases with a decrease of wood density. It is also clear that the influence of ε_y in wood stiffness for chestnut (hardwood) is much lower than for the other two species (softwoods). This phenomenon is probably a consequence of the quality of the predrilled holes described by Dias (2005). Wood with higher densities, particularly the hardwood used, permits a much tighter fitting and therefore an almost perfect contact between the steel and wood from the start of the test. Conversely, when the hole surface is not smooth, it is necessary to wait for some plastic deformation to occur before good contact between the materials is achieved. The analysis of the values in Table 2 also strengthen this conclusion, because test specimens with low yield strain ($\varepsilon_y < 0.01$) had high foundation moduli, 188.5-333.06 GPa/m. Test specimens with high yield strain values ($0.070 < \varepsilon_y < 0.13$) had much lower foundation moduli, 49.5-66.0 GPa/m.

CONCLUSIONS

The material model used in this study led to a very accurate description of the mechanical behavior of three different species of wood in embedment tests. Spruce, Maritime pine, and chestnut were all analyzed, and a single material model accounted for the differences among the species. This conclusion is supported by the stresses and load-slip curves obtained from the models that are similar to laboratory tests.

From the tests and simulation results, it was concluded that deformation in wood is significantly influenced by nonlinear phenomena, even when small loads are applied at levels generally considered as elastic. The numerical results showed that nonlinear deformations occur in the material before sufficient compression and frictional contact is achieved between wood and steel. This nonlinear phenomenon tends to obscure the influence of the elastic properties of the material in the initial loading, which is always a problem in using EN 26891 (CEN 1991). However, the effect disappears after one unloading–reloading cycle, and a strong correlation was found between the elastic properties used in the numerical models and the test loads and deformations during the cycle. Furthermore, the test specimens with higher plastic strains (in the numerical models) correspond to those with lower foundation moduli from the tests. From these results it was possible to conclude that the lower initial stiffness of the joints results from nonlinear deformations from nearly the start of loading.

The comparisons between yield stresses and mechanical properties of wood based on embedding and compression strength showed that the yield stress for the Hill criterion (Hill 1950) is lower than the embedding strength but higher than the compressive strength. The relationship between yield stress and embedding strength was found to be approximately linear for a wide range of wood densities of three wood species (380-715 kg/m^3).

From these results, it was concluded that the values of the mechanical properties of wood available in the literature (usually for design purposes) can be related with the parameters used to define the constitutive laws for FEM simulations.

ACKNOWLEDGMENTS

This work was cofinanced by the Portuguese Science and Technology Foundation (FCT) through Project POCTI/ECM/60089/2004—characterization of glued joints and behavior of timber-based glued structural composite elements.

REFERENCES

Adalian CPM (2002) Wood Model for the dynamic behaviour of wood in multiaxial compression. Holz Roh Werkst 60(6):433-439.

CEN (1991) ISO EN 26891—Timber structures—Joints made with mechanical fasteners—General principles for the determination of strength and deformation characteristics. European Committee for Standardization, Brussels, Belgium.

CEN (1993) EN 383. Timber structures—Test methods—Determination of embedding strength and foundation values for dowel type fasteners. European Committee for Standardization, Brussels, Belgium.

CEN (2003) EN 338—Structural timber—Strength classes. European Committee for Standardization, Brussels, Belgium.

Chen CJ, Lee TL, Jeng DS (2003) Finite element modeling for the mechanical behavior of dowel-type timber joints. Comput Struc 81(30-31):2731-2738.

Dias AMPG (2005) Mechanical behaviour of timber-concrete joints. PhD thesis, Delft University of Technology, Delft, The Netherlands. 293 pp.

Dias AMPG (2006) Simulation of large deformations on timber joints using 3D FEM models. Electronic edition, 14 pages *in* CA Mota Soares, JAC Martins, HC Rodrigues, JAC Ambrósio, CAB Pina, CM Mota Soares, EBR Pereira, J Folgado, eds. Proc 3rd European Conference on Computational Mechanics, Springer, Lisbon, Portugal.

Dias AMPG, Cruz HMP, Lopes SMR, Van de Kuilen JWG (2010) Stiffness of dowel-type fasteners timber-concrete joints. Proc Institute Civil Eng-Str B 163(4):257-266.

Dias AMPG, Lopes SMR, Van de Kuilen JWG, Cruz HMP (2007a) Load-carrying capacity of timber-concrete joints with dowel-type fasteners. J Struct Eng 133(5):720-727.

Dias AMPG, Van de Kuilen JW, Lopes S, Cruz H (2007b) A non-linear 3D FEM model to simulate timber–concrete joints. Adv Eng Softw 38(8-9):522-530.

FPL (1999) Wood handbook—Wood as an engineering material. Gen Tech Rep FPL-GTR-113. USDA For Serv Forest Products Laboratory, Madison, WI. 463 pp.

Fragiacomo M, Amadio C, Macorini L (2007) Short- and long-term performance of the 'Tecnaria' stud connector for timber–concrete composite beams. Mater Struct 40(10):1013-1026.

Gutkowski R, Brown K, Shigidi A, Natterer J (2008) Laboratory tests of composite wood–concrete beams. Construct Build Mater 22:1059-1066.

Hill R (1950) The mathematical theory of plasticity. Clarendon Press, Oxford, UK. 355 pp.

Kharouf N, McClure G, Smith I (2003) Elasto-plastic modeling of wood bolted connections. Comput Struc 81(8-11):747-754.

Patton-Mallory M, Cramer SM, Smith FW, Pellicane PJ (1997) Nonlinear material models for analysis of bolted wood connections. J Struct Eng 123(8):1063-1070.

Silva VD (2006) Mechanical and strength of materials. Springer-Verlag Berlin, Heidelberg, New York.

Van der Put TACM (1989) Deformation and damage processes in wood. PhD thesis, Delft University of Technology, Delft, The Netherlands. 154 pp.

APPENDIX

d = diameter of the dowel (mm)

E_{xx}, E_{yy}, E_{zz} = elasticity modulus of wood in the three principal directions (MPa)

$G_{xy}, G_{zx},$ = the distortion modulus (MPa)

ε_y = yield strain

ε_c = consolidation strain

f_h = embedding strength of wood (MPa)

k_f = foundation modulus of wood (GPa/m)

ρ = wood density (kg/m^3)

σ_0 = yield stress parallel to the grain (MPa)

σ_{90} = yield stress perpendicular to the grain (MPa)

σ_v = yield shear stress (MPa)

$\bar{\sigma}$ = yield stress (MPa)